

NMR study of the ferromagnetic phases of SmMn_2Ge_2 as a function of temperature and pressure

J. S. Lord, P. C. Riedi, and G. J. Tomka

Department of Physics and Astronomy, University of St. Andrews, St. Andrews, Fife KY16 9SS, United Kingdom

Cz. Kapusta

Department of Solid State Physics, Faculty of Physics and Nuclear Techniques, University of Mining and Metallurgy, 30-059 Cracow, Poland

K. H. J. Buschow

Van der Waals-Zeeman Laboratorium, University of Amsterdam, The Netherlands and Philips Research Laboratories, P.O. Box 80 000, NL-5600 JA Eindhoven, The Netherlands

(Received 6 July 1995)

The behavior of the reentrant ferromagnet SmMn_2Ge_2 has been studied as a function of temperature and pressure using NMR in zero applied field. At atmospheric pressure SmMn_2Ge_2 is ferromagnetic (FM) from $T_{11} \approx 348$ K to $T_{12} \approx 196$ K, then antiferromagnetic (AFM) to $T_{13} \approx 100$ K. The material is again ferromagnetic below T_{13} . The behavior of T_{13} as a function of pressure has been studied using ^{55}Mn NMR. The value of dT_{13}/dP at low pressure is found to be about -16 K kbar $^{-1}$, in agreement with earlier work but its magnitude decreases at higher pressure. The value of T_{13} at 7.8 kbar is 47 K. The ^{55}Mn NMR frequency increases with increasing temperature in the range 3–75 K, despite the decrease in magnetization by some 16%. The decrease in magnetization is attributed to the collapse of the ordered Sm state near 75 K. The ^{147}Sm and ^{149}Sm NMR could, however, only be observed up to 19 K, because of the rapid increase of the transverse relaxation rate with temperature, so we do not have conclusive evidence that the Sm moment has no influence on the AFM-FM transition at T_{13} . A remarkable feature of the Sm NMR is that its frequency at a given temperature is independent of pressure whereas the Mn NMR frequency decreases with increasing pressure.

I. INTRODUCTION

The series of compounds RMn_2Ge_2 , where R is a rare-earth or yttrium, are naturally layered compounds which recently have become of renewed interest. For example, the magnetoresistance of SmMn_2Ge_2 has been investigated to complement the studies of giant magnetoresistance effects in artificially layered magnetic/nonmagnetic superlattices grown by molecular beam epitaxy or sputtering.¹ Since their magnetic properties are sensitive to the Mn-Mn separations, the RMn_2Ge_2 compounds are also model systems for the study of the volume dependence of ferromagnetism in metals.²

The crystal structure of SmMn_2Ge_2 , as shown in Fig. 1, is of body centered tetragonal BaAl_4 type³ with the two crystallographically inequivalent Al sites occupied by Mn and Ge atoms. The atoms of each type lie on planes perpendicular to the c axis with the sequence $-\text{Mn}_2\text{-Ge-Sm-Ge-}$. The inter-layer Mn-Mn or Sm-Sm distance is much larger than the intralayer distance.

The magnetic properties of the RMn_2Ge_2 series have been reviewed by Szytula and Leciejewicz.⁴ Typically two magnetic transitions are observed as a function of temperature, because the Mn moments order in the range 300–460 K, but the R moments order only below 100 K. The phase diagram of SmMn_2Ge_2 is however more complicated than that of the other RMn_2Ge_2 compounds; see Fig. 2. At atmospheric pressure the Mn moments order at $T_{11} \approx 348$ K with a ferromagnetic (FM) configuration along the c axis $\langle 001 \rangle$. At $T_{12} \approx 196$ K there is a first order transition to an antiferro-

magnetic (AFM) state with Mn moments still lying along $\langle 001 \rangle$, and a further first order transition to a FM state ordered along $\langle 110 \rangle$ occurs at $T_{13} \approx 100$ K. On cooling the a axis contracts by $\sim 0.15\%$ at T_{12} , and expands again by the same amount at T_{13} , as investigated by Gyorgy *et al.*⁵ The

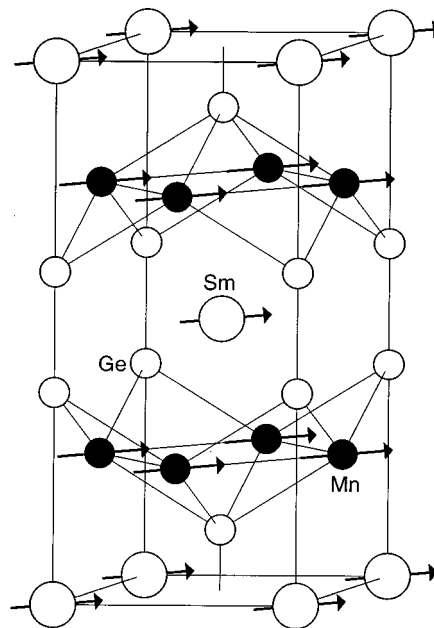


FIG. 1. Crystal structure of SmMn_2Ge_2 . The direction of moments in the low temperature ferromagnetic phase are indicated.

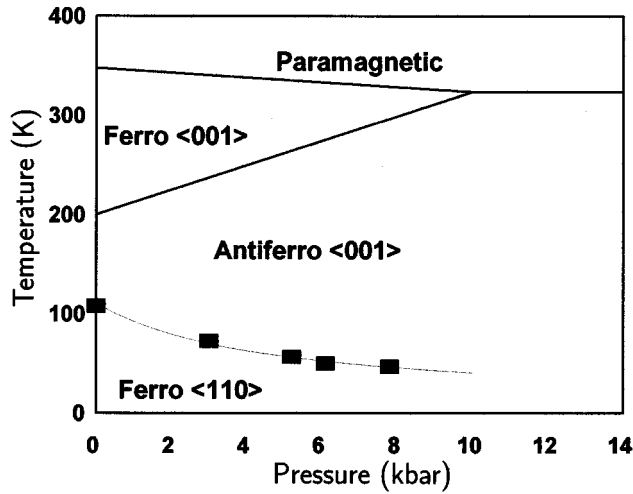


FIG. 2. T - P phase diagram for SmMn_2Ge_2 .

accuracy of their thermal expansion measurements was such that it is difficult to decide if the c axis also exhibits a jump at T_{i2} and T_{i3} but the jump is less than 0.08%.

The best value for the magnetization at 4.2 K is probably $3.8\mu_B$,⁶ although the value given in the original paper⁷ is $4.18\mu_B$. Assuming the Sm NMR frequency at 4.2 K is consistent with that of a fully polarized Sm^{3+} ion (with $g_J=2/7$, $J=5/2$, $\mu=0.71\mu_B$), so a FM coupling to the Mn leads to a Mn moment of $1.55\mu_B$ in the low temperature limit. The moment per formula unit has decreased by about $0.6\mu_B$ by 77 K. This decrease in magnetic moment could, therefore, be largely due to the collapse of the Sm moment. By 273 K the moment has dropped to $2.3\mu_B$ per formula unit.

The FM-AFM transition at T_{i2} is driven by the thermal contraction of the SmMn_2Ge_2 lattice on cooling, since FM is only observed for a planar Mn-Mn separation ≥ 0.285 nm in RMn_2Ge_2 compounds.⁴ The origin of the AFM-FM transition at T_{i3} is less clear. It was originally proposed that FM ordering of the Sm moments could drive the Mn moments from AFM to FM.⁷ Our measurements suggest that the magnetization of the Sm sublattice must be small or zero around T_{i3} at atmospheric pressure. Although this does not preclude the Sm from contributing to the transition, a mechanism driven by the ordering of the Sm sublattice seems inconsistent with the small entropy change [less than $(R/10)\ln 2$] measured by Gyorgy *et al.*⁵

In order to provide further information on the stability and origin of the low temperature FM phase of SmMn_2Ge_2 , we have carried out zero external field NMR measurements on both Sm and Mn as a function of temperature and pressure. The value of T_{i3} was taken to be the temperature at which the Mn NMR signal vanished, due to the low rf field enhancement in the AFM state. The value of T_{i3} was measured up to 7.8 kbar; see Fig. 2. The Mn NMR could also be observed in the ferromagnetic state at temperatures above T_{i2} . The Sm NMR was only observable up to 19 K, because of the rapid increase of the transverse relaxation rate with temperature.

II. EXPERIMENT

The NMR experiments were carried out in a new 10–1000 MHz phase coherent swept frequency spin echo spec-

TABLE I. The NMR frequencies of quadrupole splitting and lines, and effective fields for SmMn_2Ge_2 at atmospheric pressures.

Nucleus	T (K)	ν (MHz)	B_e (T)	$(\partial \ln \nu / \partial P)$ (Mbar) ⁻¹	ν_Q (MHz)
⁵⁵ Mn	273	144.7	-13.7		
	77	189.0	-17.9	^a	
	4.2	187.3	-17.7	-3.9	0.058
¹⁴⁷ Sm	4.2	576.6	330	<0.005	8.60
¹⁴⁹ Sm	4.2	475.6	330	(<0.04)	2.425
¹⁴⁷ Sm free ion (Refs. 10,12)		600	338		9.66
¹⁴⁹ Sm free ion (Refs. 10,12)		485	338		2.8

^aFM to AFM transition.

trometer with the sample in an untuned sample holder.⁸ The spectra were recorded by integrating the spin echo at each frequency as described previously.⁹ The low Q of the untuned sample holder meant that there was not sufficient rf power available to excite a spin echo from the ⁵⁵Mn nuclei in the AFM phase. The phase boundary at T_{i3} was taken as the temperature and pressure at which the ⁵⁵Mn signal vanished.

The high pressure experiments were carried out in a Be-Cu cell. The pressure was applied to the liquid immersed sample at room temperature and locked into the cell. The cell could then be removed from the press and cooled to low temperature. The pressure was measured using the resistance of a calibrated semiconductor transducer. The maximum pressure obtained at 3 K was 7.8 kbar.

The ⁵⁵Mn, ¹⁴⁷Sm, and ¹⁴⁹Sm frequencies measured at several temperatures and their pressure dependences are shown in Table I. For quadrupole split Sm spectra, the values in the table correspond to the central lines. The Sm frequencies were converted to an effective field, allowing for a hyperfine anomaly.¹⁰ Typical spectra are shown in Figs. 3 and Fig. 4.

III. THE PHASE DIAGRAM

At atmospheric pressure, T_{i3} , determined from the temperature at which the ⁵⁵Mn signal disappeared, was found to be 108 K. The initial decrease of T_{i3} with pressure was $dT_{i3}/dP \approx -16$ K kbar⁻¹, but the magnitude of the slope decreased rapidly at higher pressures; Fig. 2. The shape of the T_{i3} - P curve, shown in Fig. 2, is similar to that obtained by “chemical pressure” experiments involving changing the lattice constants by substituting Si for Ge or another rare-earth for Sm in SmMn_2Ge_2 .¹¹ The decrease in dT_{i3}/dP at lower values of T_{i3} is indicative of the growing importance at lower temperatures of the role played by the Sm sublattice in stabilizing the low temperature ferromagnetic $\langle 110 \rangle$ phase.

In the next two sections, we discuss the evidence from Mn and Sm NMR for the contribution from the Sm sublattice to the magnetic phase transition at T_{i3} .

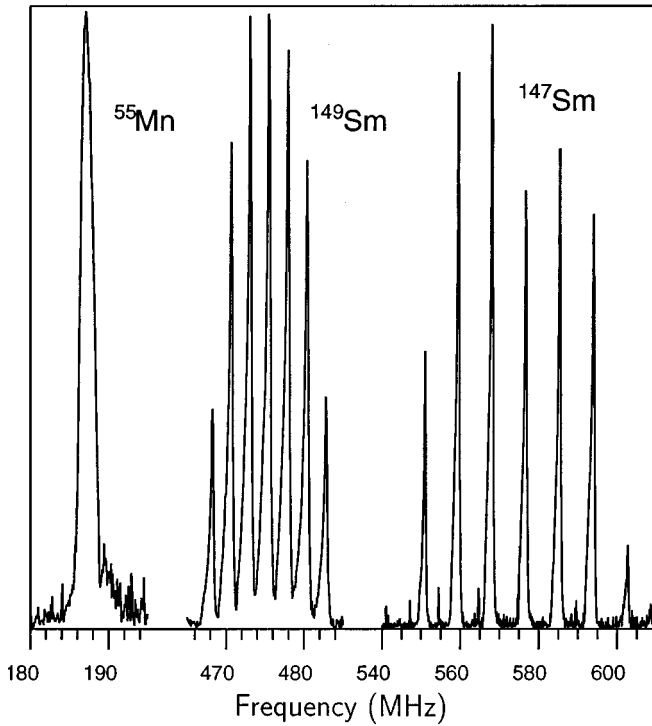


FIG. 3. NMR spectrum of SmMn_2Ge_2 at 4.2 K and at atmospheric pressure.

IV. SAMARIUM NMR

The ^{147}Sm and ^{149}Sm NMR was measured from 3–19 K at pressures up to 7.8 kbar. A typical spectrum is shown in Fig. 3. Since the Sm nuclei have spin 7/2, a seven line, quadrupole split spectrum is observed for each isotope. An unusual feature for a ferromagnetic material is that the quadrupole frequency also can be observed as a modulation on

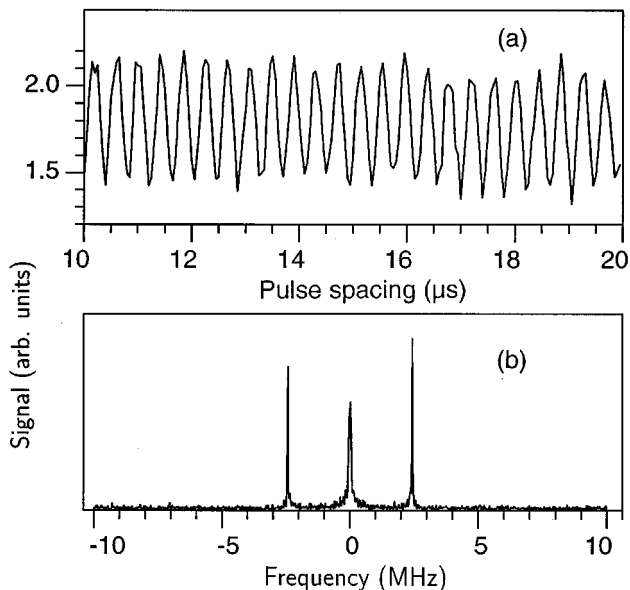


FIG. 4. (a) Modulation of the spin echo decay at 475 MHz of ^{149}Sm in SmMn_2Ge_2 at 4.2 K under zero applied pressure. (b) The Fourier transform shows a quadrupole splitting in agreement with Fig. 3.

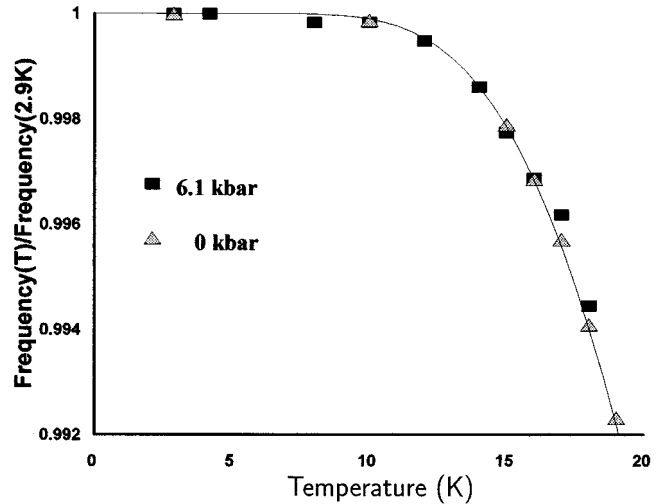


FIG. 5. Temperature dependence of the Sm NMR spectra at zero applied pressure and under 6.1 kbar. The line is given by Eq. (1) with $a=2/5$ and $b=77$ K.

the spin echo decay; see Fig. 4. Usually, as in the case of ^{55}Mn (discussed in Sec. V), the ratio of quadrupole splitting to linewidth is such that the quadrupole interaction is only observable either as a multiple line spectrum, or as a modulation on the spin echo decay. The ^{149}Sm NMR frequency is shown as a function of temperature in Fig. 5.

The effective field at the Sm nucleus in SmMn_2Ge_2 in the low temperature limit is estimated to be 330 T, which may be compared with the free Sm^{3+} ion value of 338 T.^{6,10,12} The largest contribution to the Sm effective field comes from the orbital motion of the 4*f* electrons of the parent atom which induces a field parallel to the magnetization. The 8 T discrepancy between SmMn_2Ge_2 , and the free Sm^{3+} ion value presumably arises from a transferred effective field from the Mn moments.

We assume that the change of the ^{149}Sm NMR frequency is a measure of the Sm moment and that the small contribution from the Mn magnetization remains unchanged over the range 3–19 K. Above 19 K the transverse relaxation time T_2 is too short for a signal to be observed. Since the Sm NMR frequency has only changed by about 1% by 19 K, it is not possible to extrapolate the data reliably to find the temperature T_c at which the Sm moment collapses. The simplest approach is to use the low temperature limit of mean field theory and write

$$\nu = \nu_0(1 - ae^{-b/T}), \quad (1)$$

where $a=1/J$ and $b=3T_c/(J+1)$. A good fit to the measurements has the form $a=0.99$ and $b=92$ K, but an imposed fit with $a=1/J=2/5$ leads to $b=77$ K.

The mean field value of T_c is therefore around 100 K, i.e., quite close to T_{f3} in Fig. 1. Since the material exhibits a large magnetocrystalline anisotropy at low temperatures, the resulting large energy gap in the spin wave spectrum means that it is reasonable to fit the temperature dependence of the Sm NMR frequency to a mean field theory, as shown by the line in Fig. 5. At 4.2(26) K, the magnetization

measurements⁷ extrapolate to an anisotropy field of some 24(18) T which is equivalent to a 4(3) K gap in the spin-wave spectrum.

The Sm NMR frequency, Fig. 5, was found to be independent of pressure in the temperature range 3–19 K. The change in the frequency with pressure throughout this range of temperatures was less than 5×10^{-5} kbar⁻¹ in $(\partial \ln \nu / \partial P)$. This is a very surprising result, since T_{i3} has decreased from 108 K at atmospheric pressure to 47 K at 7.8 kbar, and the Mn frequency, which is roughly proportional to the moment on the Mn site, also decreases under pressure. The Mn moment, assumed to be proportional to the ⁵⁵Mn NMR frequency, decreases by 2.4% by 7.8 kbar. Assuming that the 8 T discrepancy in the effective field at the Sm nucleus is indeed caused by the transferred field from the Mn, we would estimate that $(\partial \ln \nu / \partial P) \approx +8 \times 10^{-5}$ kbar⁻¹. It seems likely, therefore, that the decrease in the Mn moment is largely being compensated by a decrease in the Mn-Sm distance.

The quadrupole splitting ν_Q of the ¹⁴⁷Sm(¹⁴⁹Sm) NMR at 4.2 K, 8.6(2.4) MHz, is significantly less than the free ion values of 9.7(2.8) MHz, showing that the lattice contribution to the electric field gradient has the opposite sign to the dominant $4f$ contribution. The value of $(\partial \ln \nu_Q / \partial P)$ was estimated to be less than 3×10^{-5} kbar⁻¹, which is consistent with our estimate of 1×10^{-5} kbar⁻¹ if we assume that only the lattice contribution changes with pressure and that the compressibility is isotropic.

The “lattice” electric field gradient (EFG) includes the on-site contribution from the $6p$ and $5d$ -like electrons and the contribution from the charge distribution at neighboring sites. Recently it was found that for many RE (rare-earth) $3d$ metal compounds, the on-site contribution to the lattice EFG dominates.¹³

For the Sm site in SmMn₂Ge₂, the fourfold tetragonal c axis is the highest symmetry axis. Thus the lattice EFG is axially symmetric along it and its c axis component $V_{cc}(\text{latt})$ is related to the in-plane component $V_{pp}(\text{latt})$ according to Laplace’s equation: $V_{cc}(\text{latt}) = -2V_{pp}(\text{latt})$. The value of the quadrupole splitting, measured in the NMR experiment, corresponds to the EFG component along the effective field in the plane perpendicular to the c axis. As the value of the effective field is close to that of the free ion, it means that Sm is in its fully polarized state $J_z = J = 5/2$. In the recent study of Sm₂Fe₁₇N_x,¹⁴ it was found that, in the fully polarized state of Sm, the value of the $4f$ contribution in the crystal was -249×10^{20} V m⁻² which is 20% larger in magnitude than that of the free ion. The effect was attributed to a contraction of the $4f$ shell of the crystal from that of the free ion. Taking the value as an estimate for the $4f$ electron contribution in SmMn₂Ge₂ we arrive at the $V_{pp}(\text{latt})$ value of 52.5×10^{20} V m⁻² and the $V_{cc}(\text{latt})$ value of -105×10^{20} V m⁻².

A very high planar anisotropy of the compound at low temperatures ($B_a = 24$ T) originates from the interaction of Sm $4f$ electrons with the crystal electric field (CEF). Its lowest order term corresponds to the interaction of the quadrupole moment of the $4f$ shell with the EFG, produced mainly by the asphericity of the $5d$ and $6p$ electron shells of the parent atom. This asphericity is the result of the presence of neighbors in the lattice.¹³ The CEF coefficient A_2^0 , used in

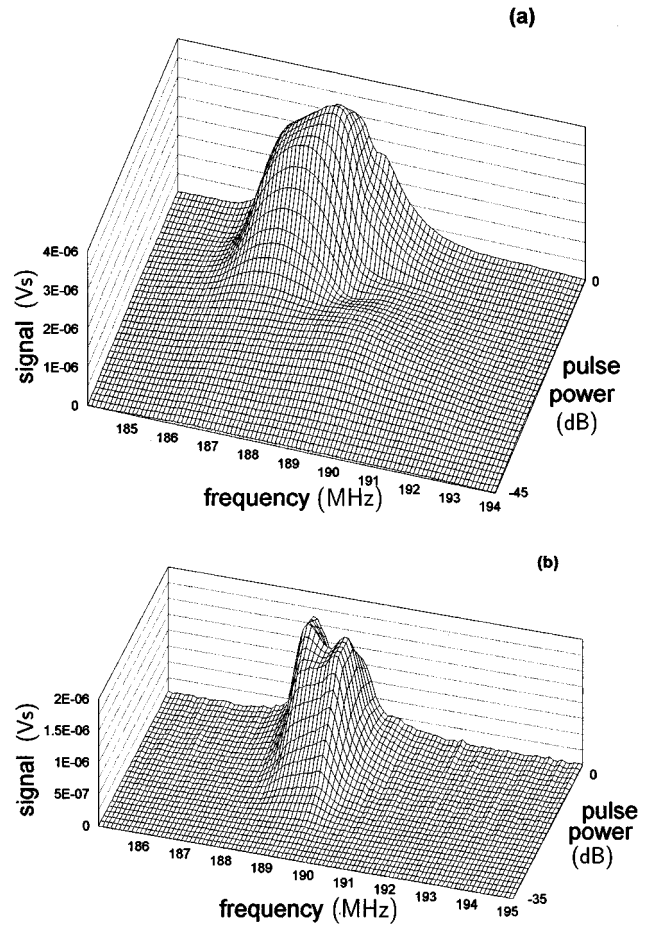


FIG. 6. Variation of the ⁵⁵Mn NMR spectrum with power under zero applied pressure (a) at 4.2 K and (b) at 77 K.

the CEF formalism, is proportional to this EFG. A lack of a strict relation between the EFG at the nucleus and the EFG exerted by the $4f$ shell means that only an approximate relation can be used:

$$A_2^0 = -D/4eV_{cc}(\text{latt}). \quad (2)$$

The relation, however, holds for many RE intermetallic compounds. Taking the value of $1/320$ for the coefficient D , as obtained from a comparison of a Mössbauer spectroscopy study with bulk magnetic data for Gd₂Fe₁₇ and other RE- $3d$ intermetallics,¹⁵ the CEF coefficient A_2^0 is $266 \text{ K } a_0^{-2}$, where a_0 is the Bohr radius. The value is very close in magnitude to that of $-242 \text{ K } a_0^{-2}$ reported for Sm₂Fe₁₇N_x,¹⁶ a permanent magnet material with a strong uniaxial anisotropy in which the lowest order anisotropy contribution related to A_2^0 dominates. Its anisotropy field B_a of 23 T is also very close to that of 24 T for SmMn₂Ge₂. This indicates that the contribution related to A_2^0 is also dominant here.

V. MANGANESE NMR

The ⁵⁵Mn NMR spectrum consists of a single line at lower pulse powers but develops additional structure at lower frequencies as the power is increased, as shown in Fig. 6(a) at 4.2 K and Fig. 6(b) at 77 K. At low pulse powers signals arise from domain wall enhancement caused by the

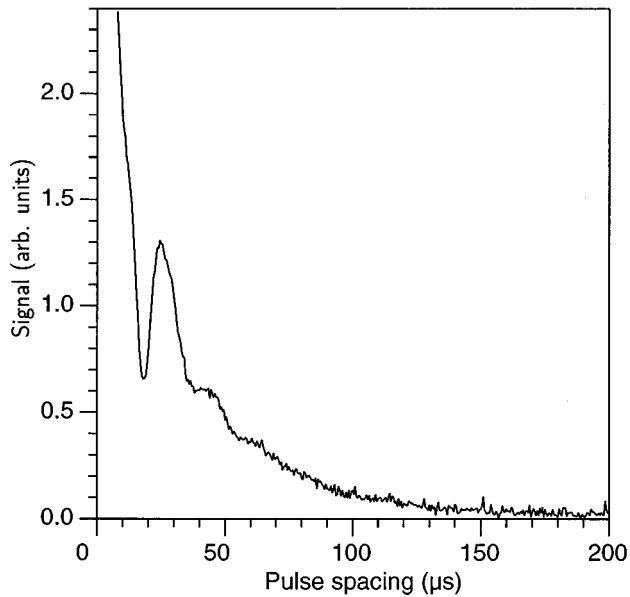


FIG. 7. Spin echo decay of ^{55}Mn at atmospheric pressure and at 4.2 K. The modulation reflects a quadrupole splitting of 60 kHz.

rotation of moments at the center of the domain wall. At the center of the wall small domain wall movements result in the largest moment rotation. At higher pulse powers, moments at the domain wall edge contribute to the enhanced NMR signal. These moments are, in general, in a different magnetocrystalline environment from the moments at the domain wall center and so experience a different effective field, resulting in the more complicated line structure observed at higher pulse powers.

The ^{55}Mn spin is $5/2$, but no quadrupole structure is apparent in the swept frequency spectrum. A small quadrupole splitting is, however, observable via the modulation of the spin echo decay; see Fig. 7 and Table I. The calculated quadrupole splitting (60 kHz) is much less than the linewidth of the inhomogeneously broadened line (1–3 MHz).

The ^{55}Mn NMR frequency in the low temperature limit is 187.3 MHz at atmospheric pressure and tends to decrease with increasing pressure; see Fig. 8. Since the effective field at the Mn nucleus arises largely from the moment at the Mn

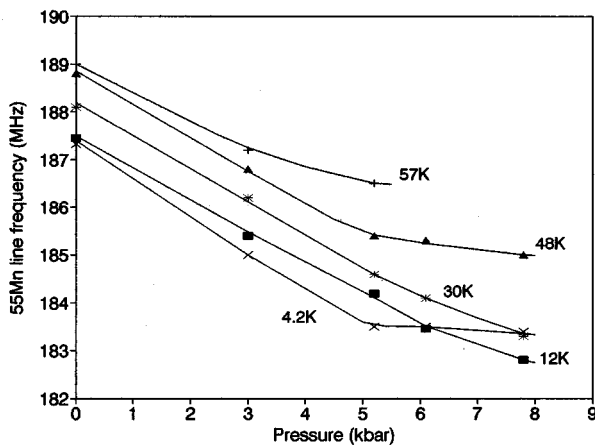


FIG. 8. Variation of ^{55}Mn frequency with pressure at various temperatures.

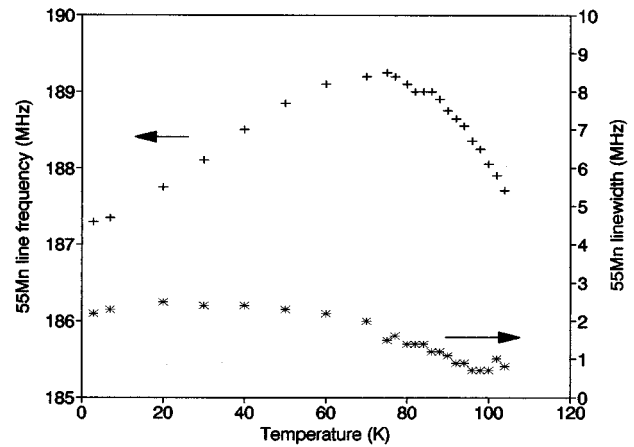


FIG. 9. Variation of ^{55}Mn frequency with temperature at atmospheric pressure. Changes in the linewidth are also shown.

site, the decrease in the NMR frequency shows that the magnetization of SmMn_2Ge_2 decreases under pressure. This is consistent with the fact that the unit cell of SmMn_2Ge_2 increases with decreasing temperature through the transition at T_{13} and that in general a large Mn-Mn spacing is essential for ferromagnetism in RMn_2Ge_2 . The change of slope of the ^{55}Mn NMR frequency with pressure above 5 kbar shown in Fig. 8 may, in part, be due to a pressure dependence of the spectrum shown in Fig. 6(b), but it is interesting to note that in Fig. 2 for pressures above 5 kbar the rate of change of T_{13} is also smaller than at lower pressures.

At atmospheric pressure and at low temperatures, the Mn NMR frequency initially increases with temperature. The maximum NMR frequency of 189.3 MHz occurs around 75 K then decreases to 187.7 MHz at T_{13} , as shown in Fig. 9. The data in Fig. 9 indicate the frequency of the center of the ^{55}Mn NMR spectrum at a pulse power corresponding to an attenuation of 12 dB in Fig. 6. For this pulse power there is a good signal to noise ratio, and the ^{55}Mn NMR spectrum has a single peak at low temperatures. This pulse power was chosen, as the form of the spectrum changes little with temperature and thus provides a good representation of changes in value of the ^{55}Mn frequency. Since the magnetization decreases by $0.6\mu_B$ between low temperature and 77 K, which is comparable to the Sm ground state moment of $0.7\mu_B$, the increase in the Mn frequency up to 75 K is attributed to the decrease of a transferred hyperfine field from the Sm. (The transferred hyperfine field from the Sm is positive with respect to the Mn moment direction, whereas the contact interaction with the Mn spin of the parent atom induces a predominantly negative hyperfine field at the Mn nucleus, i.e., antiparallel to the magnetization).

A further indication that the Sm moment has collapsed by 75 K is provided by the temperature dependence of the Mn NMR linewidth; see Fig. 9. The change of the linewidth with temperature appears to follow the change of Sm moment. In the high temperature FM phase, where the Sm moment is certainly zero, the linewidth is 1 MHz. The slow decrease in the ^{55}Mn linewidth over the range 70–100 K may reflect a significant paramagnetic Sm magnetization induced via the exchange interaction with the Mn. It is possible that the large changes in ^{55}Mn NMR frequency and linewidth at low temperatures are also related to changes in the magnetic struc-

ture of the Mn sublattice. Since the Mn moments are aligned along the c axis in the higher temperature ferromagnetic and antiferromagnetic phases, it seems likely that the Mn sublattice below T_{13} may also prefer to align along the c axis. Despite this, a resultant alignment along the $\langle 110 \rangle$ direction is imposed by the much stronger anisotropy of the Sm. However, since this is likely to be a hard direction for Mn, the Mn moments may tilt out of the plane, resulting in a noncollinearity between Sm and Mn moments. The anisotropy of SmMn_2Ge_2 is strongly dependent on the temperature⁷ below T_{13} . As this anisotropy arises predominantly from the Sm sublattice, it will have a strong effect on any tendency for the Mn moments to tilt out of the $\{001\}$ plane. Such changes appear to be reflected in changes in the c axis magnetization measured in a 2 kOe field as a function of temperature by Gyorgy *et al.*⁵ Their measurements are strikingly similar to our measurements of the changes in ^{55}Mn NMR frequency with temperature, shown in Fig. 9.

VI. CONCLUSIONS

Our investigation of the behavior of the reentrant ferromagnet SmMn_2Ge_2 , as a function of temperature and pressure using NMR, has produced interesting results in the ferromagnetic region below the transition temperature T_{13} . At low pressure, dT_{13}/dP was found to be about -16 K kbar^{-1} , but its magnitude decreased at higher pressure, indicative of the Sm sublattice stabilizing the ferromagnetic phase at lower temperatures. Another indication of this was the value of the CEF coefficient, $A_2^0 = 266 \text{ K } a_0^{-2}$. This is

close in magnitude to A_2^0 in $\text{Sm}_2\text{Fe}_{17}\text{N}_x$ in which the anisotropy is dominated by the Sm sublattice. Extrapolation of low temperature Sm NMR data using mean field theory indicated that, at $T_{13} \approx 100 \text{ K}$ and atmospheric pressure, the magnetization of the Sm sublattice was small or zero. This conclusion is supported by a measured increase of the ^{55}Mn NMR frequency with temperature up to 75 K, which we have attributed to a decrease in the transferred hyperfine field from Sm, as the magnetization of the Sm sublattice drops to zero near 75 K. The observed decrease in ^{55}Mn linewidth over the range 70–100 K may reflect a significant paramagnetic Sm magnetization, which could play a role in driving the transition at T_{13} .

It has been observed that the ^{55}Mn NMR frequency tended to decrease as a function of pressure, with $\partial \ln \nu / \partial P = -3.9 \text{ Mbar}^{-1}$ at 4.2 K and atmospheric pressure, reflecting a decrease in moment at the Mn site. It is therefore surprising that the Sm NMR frequency at a given temperature was found to be independent of pressure. We suggest that the decrease in transferred field at the Sm nucleus with pressure may be compensated by a decrease in the Mn-Sm distance, which would leave the effective field at the Sm unchanged.

ACKNOWLEDGMENTS

The financial support of the SERC/EPSRC is gratefully acknowledged. One of us (Cz.K.) acknowledges the support of the Leverhulme Trust during his stay at St. Andrews.

- ¹M. J. Hall, B. J. Hickey, M. A. Howson, M. J. Walker, J. Xu, D. Greig, and N. Wiser, *Phys. Rev. B* **47**, 12 785 (1993).
- ²J. H. V. J. Brabers, A. J. Nolten, F. Kayzel, S. H. J. Lenczowski, K. H. J. Buschow, and F. R. de Boer, *Phys. Rev. B* **50**, 16 410 (1994).
- ³W. Rieger and E. Parthe, *Mh. Chem.* **100**, 444 (1969).
- ⁴A. Szytula and J. Leciewicz, in *Handbook on the Physics and Chemistry of the Rare Earths, Vol. 12*, edited by K. A. Gschneidner, Jr. and L. Eyring (Elsevier, Amsterdam, 1989), p. 133.
- ⁵E. M. Gyorgy, B. Batlogg, J. P. Remeika, R. B. van Dover, R. M. Fleming, H. E. Bair, G. P. Espinosa, A. S. Cooper, and R. G. Maines, *J. Appl. Phys.* **61**, 4237 (1987).
- ⁶J. S. Lord, P. C. Riedi, Cz. Kapusta, and K. H. J. Buschow, *Physica B* **206& 207**, 383 (1995).
- ⁷H. Fujii, T. Okamoto, T. Shigeoka, and N. Iwata, *Solid State Commun.* **53**, 715 (1985).

- ⁸J. S. Lord and P. C. Riedi, *Meas. Sci. Technol.* **6**, 149 (1995).
- ⁹T. Dumelow and P. C. Riedi, *Hyperfine Interact.* **35**, 1061 (1987).
- ¹⁰H. Figiel, Cz. Kapusta, N. Spiridis, G. Stoch, P. C. Riedi, and M. Rosenberg, *J. Magn. Magn. Mater.* **104-107**, 1198 (1992).
- ¹¹R. Duraj, M. Duraj, and A. Szytula, *J. Magn. Magn. Mater.* **82**, 319 (1989); R. Duraj, M. Duraj, and A. Szytula (unpublished).
- ¹²B. Bleaney, in *Magnetic Properties of Rare Earth Metals*, edited by J. R. Elliot (Plenum Press, New York, 1972), Chap. 8.
- ¹³R. Coehoorn and K. H. J. Buschow, *J. Appl. Phys.* **69**, 5590 (1991).
- ¹⁴Cz. Kapusta, M. Rosenberg, P. C. Riedi, M. Katter, and L. Schultz, *J. Magn. Magn. Mater.* **134**, 106 (1994).
- ¹⁵P. C. M. Gubbens, A. M. van der Kraan, and K. H. J. Buschow, *Hyperfine Interact.* **53**, 37 (1989).
- ¹⁶Hong-Shuo Li and J. M. D. Coey, *J. Magn. Magn. Mater.* **115**, 152 (1992).